

Lunar volatile depletion due to incomplete accretion within an impact-generated disk

Robin M. Canup^{1*}, Channon Visscher^{1,2}, Julien Salmon¹ and Bruce Fegley Jr³

The Moon may have formed from an Earth-orbiting disk of vapour and melt produced by a giant impact¹. The mantles of the Moon and Earth have similar compositions. However, it is unclear why lunar samples are more depleted in volatile elements than terrestrial mantle rocks^{2,3}, given that an evaporative escape mechanism4 seems inconsistent with expected disk conditions⁵. Dynamical models^{6,7} suggest that the Moon initially accreted from the outermost disk, but later acquired up to 60% of its mass from melt originating from the inner disk. Here we combine dynamical, thermal and chemical models to show that volatile depletion in the Moon can be explained by preferential accretion of volatile-rich melt in the inner disk to the Earth, rather than to the growing Moon. Melt in the inner disk is initially hot and volatile poor, but volatiles condense as the disk cools. In our simulations, the delivery of inner disk melt to the Moon effectively ceases when gravitational interactions cause the Moon's orbit to expand away from the disk, and this termination of lunar accretion occurs before condensation of potassium and more volatile elements. Thus, the portion of the Moon derived from the inner disk is expected to be volatile depleted. We suggest that this mechanism may explain part or all of the Moon's volatile depletion, depending on the degree of mixing within the lunar interior.

The Moon and the bulk silicate Earth (BSE) share many compositional similarities, including comparable abundances of refractory elements³ and essentially identical isotopic compositions for many elements⁸. However, it has been known since the return of Apollo samples that, compared with the BSE, the Moon is more depleted in volatile elements having condensation temperatures <1,100 K in reference solar nebula conditions, including moderately volatile potassium and sodium, as well as more highly volatile elements, including zinc^{2,3}.

The origin of this depletion is poorly understood, and there are no quantitative models of how the Moon's observed pattern of depletion emerged. It seems unlikely to have been inherited from the Moon-forming impactor, because the compositional similarities between the Moon and Earth seem to require a disk with a BSE-like composition^{1.8}. Alternatively volatiles in the protolunar material may have evaporatively escaped⁹⁻¹¹. Zinc has been cited as evidence of this, because lunar samples show an $\sim 1.1\%$ enrichment in the heavier ⁶⁶Zn isotope compared to terrestrial or martian samples, suggestive of Rayleigh fractionation during evaporation into a vacuum^{4,11}. However, the velocities required for escape from the disk exceed those expected for heavy vapour species such as Zn. These might instead escape hydrodynamically if carried by a flow of lighter species¹⁰, but even the escape of hydrogen may be minimal owing to frequent collisions with heavier species⁵.

In the limit of no escape and a closed system, a depletion could instead result if disk volatiles were preferentially accreted by the Earth rather than by the Moon. Taylor *et al.*² advocated that the lunar depletion pattern is most consistent with incomplete condensation from an initially high-temperature vapour, wherein the accretion of condensates by the Moon is 'cut off' at a characteristic temperature that allows incorporation of a small component of alkalis (for example, K and Na) but only a tiny fraction of more volatile elements (for example, Zn). Neither the mechanism that would produce such a cutoff, nor what the relevant cutoff temperature would be in an oxygen-rich protolunar disk environment¹², were known. Here we combine dynamical^{6,7}, thermal¹³ and chemical¹² models to show that the disk's evolution naturally provides a cutoff at temperatures consistent with the Moon's depletion pattern.

An initial impact-generated disk is probably a two-phase mixture of silicate vapour and melt^{1,13–15}. The disk lies within and beyond the Roche limit, located at about 3 Earth radii^{1,15}. The disk is massive, and so is vulnerable to clumping as a result of local gravitational instability^{14,16,17}. Exterior to the Roche limit (the 'outer disk'), melt clumps are gravitationally stable and mutually accrete into a moon(s)^{6,7,17}. Interior to the Roche limit (the 'inner disk'), clumps are continually sheared apart by Earth's tidal force, producing a viscosity that causes the disk to spread^{14,16}.

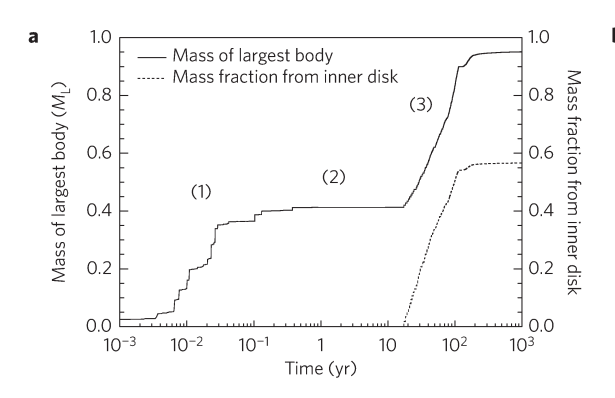
The inner disk is initially hotter than the outer disk, and it cools more slowly owing to its smaller surface area and the local production of heat via viscous dissipation^{5,6}. As a result, the inner disk may be regulated by the two-phase silicate equilibrium for $\sim 10^2$ years^{13,14,17}. During this period, the disk's surface density (σ_T), mid-plane temperature (T_c), and gas mass fraction of its atmosphere at the mid-plane (x_c) are related as¹³

$$\sigma_T \approx \left(\frac{\pi}{x_c}\right)^{1/2} \frac{\overline{\mu} P_c H}{R T_c} \left[1 + \left(\frac{C_s T_c}{x_c l} - 2\right) \frac{T_c}{T_0} \right]^{-1/2} \tag{1}$$

where $\overline{\mu}\approx 30\,\mathrm{g\,mol^{-1}}$ is the effective molecular weight of the vapour, $P_c=P_0\mathrm{e}^{-T_0/T_c}$ is the mid-plane pressure (with $P_0=3.2\times 10^{14}$ dyne cm⁻² and $T_0=6.0\times 10^4\,\mathrm{K}$; ref. 14), $H=(2R\,T_c/\overline{\mu})^{1/2}/\Omega$ (where R is the gas constant and Ω is orbital frequency), $C_s\approx 10^7\,\mathrm{erg\,g^{-1}\,K^{-1}}$ is the melt's specific heat, and $l=1.7\times 10^{11}\,\mathrm{erg\,g^{-1}}$ is the latent heat of vaporization. A gas-poor structure with $x_c\sim O(10^{-2})$ is possible¹⁴, although recent work^{13,17} argues that a stratified disk with a mid-plane melt layer surrounded by a vapour-rich atmosphere having $O(10^{-1})\leq x_c\leq 1$ is more likely (see Methods).

With time, radiative cooling from the upper and lower surfaces of the disk's atmosphere allows increased condensation, and σ_T decreases as the disk spreads¹⁷. Once σ_T falls below $\sim 10^6 \, \mathrm{g \, cm^{-2}}$,

¹Planetary Sciences Directorate, Southwest Research Institute, Boulder, Colorado 80302, USA. ²Chemistry and Planetary Sciences, Dordt College, Sioux Center, Iowa 51250, USA. ³Department of Earth and Planetary Sciences and McDonnell Center for Space Sciences, Washington University, St Louis, Missouri 63130, USA. *e-mail: robin@boulder.swri.edu



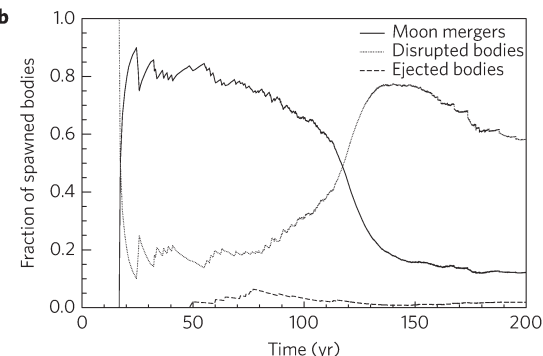


Figure 1 | **Simulation of the Moon's accretion, reproduced from ref. 6. a**, Moon mass versus time. Outer disk material rapidly accretes into a moonlet containing \sim 40% of the lunar mass (M_L) (1), and then accretion stalls (2). After \sim 20 yr, inner disk melt spreads beyond the Roche limit and supplies the final 60% of the Moon's mass (3). **b**, Fate of inner disk clumps spawned near the Roche limit versus time. Initially clumps efficiently merge with the Moon ('moon mergers'). A cutoff occurs at \sim 120 yr. Subsequently most are scattered inwards, tidally disrupted and accreted by the Earth ('disrupted bodies'). A small fraction are ejected from the system ('ejected bodies').

the inner disk's silicate vapour may fully condense^{6,17}. Subsequently, $T_{\rm c}$ probably reflects a balance between viscous dissipation in the mid-plane melt layer, cooling from the surfaces of a volatile-rich atmosphere, and heating of the atmosphere by the Earth's luminosity (see Methods).

Dynamical simulations^{6,7} predict that the first 40% or more of the Moon's mass accumulates rapidly from material initially in the outer disk (Fig. 1a(1)). Over a longer, approximately 10² yr timescale, the inner disk spreads and supplies the remainder of the Moon's mass in the form of clumps that form near the Roche limit (Fig. 1a(3))⁶. Initially the orbits of such clumps are rapidly driven outwards as a result of resonant interactions with the inner disk, allowing them to be efficiently accreted by the Moon (Fig. 1b)6. However, as the inner disk dissipates, disk torques weaken, and clumps are instead scattered onto high-eccentricity orbits by the Moon⁶. Most are then tidally disrupted as their perigees near the Earth's surface before they can accrete onto the Moon. This effect increases with time as the Moon's orbit expands, owing to both disk torques and repeated scattering events⁶. The result is a relatively abrupt transition from an accretionary regime—in which the Moon in this case gains 60% of its mass from the inner disk—to a non-accretionary regime—in which clumps originating near the Roche limit contribute little total mass to the Moon (Fig. 1b).

To evaluate the composition of melt clumps formed near the Roche limit, we consider a BSE-composition disk and perform thermodynamic equilibrium calculations using the MAGMA code^{18,19}. The composition of the melt and coexisting vapour are estimated as a function of T_c for a number of melt and gas species¹². From this we derive the partial vapour pressure of each species, which, in combination with the total bulk elemental inventory of the disk, is used to estimate the relative fraction of each element in the vapour versus melt phase as a function of T_c and σ_T (see Methods). Clumps that form rapidly through gravitational instability just outside the Roche limit are large (\gg km) for relevant values of σ_T (for example, ref. 6), and as such we assume they retain their initial composition as their orbits subsequently evolve.

Figure 2 shows the predicted degree of vaporization as a function of T_c and σ_T at the Roche limit. The 50% condensation temperatures for Zn, Na and K are given approximately by

$$T_{50}(K) \approx \frac{A}{\log(\sigma_T) - B}$$
 (2)

where σ_T is in g cm⁻² and $(A,B) = (-1.33 \times 10^4, 12.8), (-1.69 \times 10^4, 12.3)$ and $(-1.59 \times 10^4, 11.5)$ are fitting coefficients for Zn, Na and K, respectively, derived across the ranges $1 < \log(\sigma_T) < 8$

and 1000 < T (K) < 6,000. These condensation temperatures are much higher than reference solar nebula values²⁰. Equations (1) and (2) imply that for $2 \times 10^7 \ge \sigma_T ({\rm g \ cm^{-2}}) \ge 10^6$ (corresponding to a uniform surface density inner disk containing between 2.6 and 0.13 lunar masses) and $0.01 \le x_c \le 1$, the ratio of the midplane temperature at the Roche limit to the 50% condensation temperature, (T_c/T_{50}), will be between 0.98 and 1.2 for K, 1.1 and 1.3 for Na, and 1.5 and 1.8 for Zn, with a relative volatility sequence $K \le Na < Zn$. Thus while the inner disk is regulated by the silicate two-phase equilibrium, clumps near the Roche limit will be substantially depleted in K and Na, and extremely depleted in Zn.

Figure 3a shows the evolution of the inner disk surface density from the Fig. 1 simulation. Figure 3b compares the estimated midplane temperature at the Roche limit for plausible values for x_c to the 50% condensation temperatures from equation (2). The predicted clump formation temperature remains near or above T_{50} for K until the Moon has completed >98% of its accretion (Fig. 3c) and the efficiency of clump accretion by the Moon has decreased to \sim 10% (Fig. 1b). The fraction of the Moon's mass derived from the inner disk depends on the initial radial distribution of disk mass^{6,7}, but in all cases (Supplementary Methods) the cutoff in the Moon's accretion of inner disk material occurs at temperatures comparable to or somewhat higher than T_{50} for K. This is consistent both with the observed depletion of K and more volatile elements, and with the lack of depletion of elements substantially less volatile than potassium.

The cutoff mechanism we identify causes the portion of the Moon derived from the inner disk to be volatile-poor. The volatile content of the portion of the Moon derived from the outer disk is unclear. Rapid escape of an outer silicate two-phase atmosphere might occur²¹, although perhaps only for overly idealized conditions. In the absence of escape, the first portion of the Moon to form could be volatile-rich, followed by the later accumulation of an overlying 100 to 500 km volatile-poor layer derived from the inner disk. The Moon's observed depletion pattern would then be a function of the degree of mixing between these two reservoirs, which is uncertain.

In the limit of no volatile escape in the outer disk and a well-mixed lunar interior, removal of an element in the final \leq 60% Moon's mass would result in at most a factor of 2.5 depletion in the bulk Moon relative to the BSE. This is broadly similar to estimated depletions for K and Na, but much smaller than the observed depletion factor of \geq 30 for Zn (Fig. 2b). It is, however, plausible that internal mixing in the Moon was incomplete. Some evidence suggests that the initial Moon was not fully molten, with a \sim 200 to 1,000-km deep magma ocean²² that overlaid a perhaps cooler, sub-solidus interior²³. The Moon's composition as inferred from

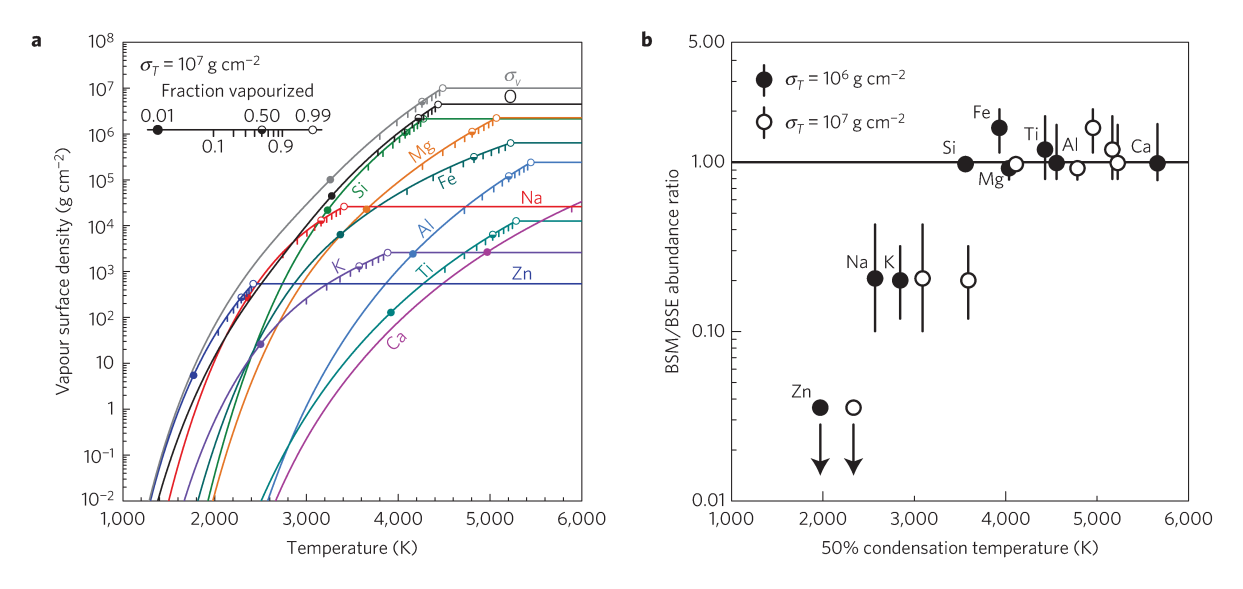


Figure 2 | **Melt-vapour equilibria in a BSE-composition protolunar disk. a**, Vapour surface density of each element and the total vapour surface density (σ_v) as a function of temperature at the Roche limit for $\sigma_T = 10^7$ g cm⁻². Vertical marks indicate mass fraction in the vapour phase from 0.1 to 0.9; symbols indicate 1% (filled circle), 50% (half-filled circle) and 99% (open circle) vaporization. **b**, Observed bulk silicate Moon (BSM), scaled to BSE abundances (with values from ref. 12 and references therein), versus T_{50} (50% condensation temperature) values for $\sigma_T = 10^6$ and 10^7 g cm⁻². Horizontal line indicates equal abundances. Arrows for Zn reflect more recent estimates^{3,26}.

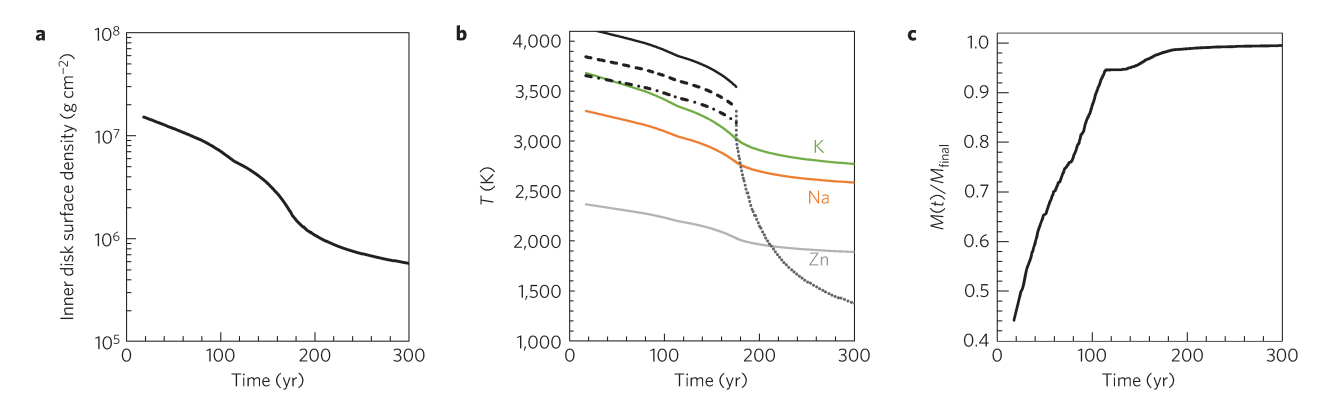


Figure 3 | Clump formation temperature and volatile content. **a**, Inner disk surface density (σ_T) versus time from the Fig. 1 simulation. **b**, Mid-plane temperature (T) at the Roche limit versus time. Solid, dashed and dot-dashed lines use equation (1) with $x_c = 1$, 0.1 and 0.01, respectively, and $\sigma_T(t)$ from **a**. Dotted curve assumes $\kappa \sigma_V = 10$, $T_{\bigoplus} = 2,300 \text{ K}$, $\beta = 0.3$ and $c/r\Omega = 0.2$ (see Methods). Green, orange and grey curves show estimated T_{50} values (equation (2)). **c**, The Moon's mass (M(t)) scaled to its final mass (M_{final}) from the Fig. 1 simulation. The Moon accretes only approximately 1% of its mass after T_c falls substantially below T_{50} for potassium.

samples (that is, mare basalts) reflects only its upper few hundred kilometres²⁴. If interior mixing was incomplete, this material would predominantly reflect the depleted, late-added material from the inner disk, with a much larger depletion factor than the well-mixed case. It is also possible that Zn and more volatile elements were further depleted by a secondary process (for example, later volcanic degassing on the Moon²⁵), implying an initial lunar Zn abundance higher than shown in Fig. 2b²⁵.

Lunar samples exhibit a mass-dependent fractionation in Zn compared to the BSE (ref. 4). In a closed system, equilibrium condensation can enrich the condensate in heavier isotopes compared to the vapour phase, although the degree of fractionation is less than can be achieved through evaporation into a vacuum. Whether the observed isotopic fractionation in Zn can be explained by a closed disk model or would require a subsequent process (for example, magma ocean outgassing¹¹) is an open issue.

We have modelled an anhydrous disk¹². The presence of water²⁵ would not change our overall conclusions: it is the silicate two-phase equilibrium that sets the disk's oxygen fugacity and thermal

structure as the Moon accretes inner disk material 12 , and Zn(g) will remain the major Zn-bearing gas even in the presence of water vapour. Results here imply that the final portion of the Moon derived from inner disk melt would be very water-poor compared to the disk's total water content, reflecting the limited solubility of H_2O in magmas at relevant disk pressures 9,12 .

Methods

Methods and any associated references are available in the online version of the paper.

Received 29 May 2015; accepted 29 September 2015; published online 9 November 2015

References

- Canup, R. M. Lunar-forming impacts: Processes and alternatives. *Phil. Trans. R. Soc. A* 372, 20130175 (2014).
- Taylor, S. R., Taylor, G. J. & Taylor, L. A. The Moon: A Taylor perspective. Geochim. Cosmochim. Acta 70, 5904–5918 (2006).

LETTERS NATURE GEOSCIENCE DOI: 10.1038/NGE02574

- 3. Taylor, G. J. & Wieczorek, M. A. Lunar bulk chemical composition: A post-Gravity Recovery and Interior Laboratory reassessment. *Phil. Trans. R. Soc. A* **372**, 20130242 (2014).
- Paniello, R. C., Day, J. M. D. & Moynier, F. Zinc isotopic evidence for the origin of the Moon. *Nature* 490, 376–379 (2012).
- 5. Nakajima, M. & Stevenson, D. J. Hydrodynamic escape does not prevent the "Wet" Moon formation. In *Proc. 45th Lunar Planet. Sci. Conf.* 2770 (2014).
- Salmon, J. & Canup, R. M. Lunar accretion from a Roche-interior fluid disk. Astrophys. J. 760, 83 (2012).
- Salmon, J. & Canup, R. M. Accretion of the Moon from non-canonical discs. Phil. Trans. R. Soc. A 372, 20130256 (2014).
- 8. Dauphas, N., Burkhardt, C., Warren, P. H. & Teng, F.-Z. Geochemical arguments for an Earth-like Moon-forming impactor. *Phil. Trans. R. Soc. A* **372**, 20130244 (2014).
- Desch, S. J. & Taylor, G. J. A Model of the Moon's Volatile depletion. In Proc. 42nd Lunar Planet. Sci. Conf. 2005 (2011).
- Desch, S. J. & Taylor, G. J. Isotopic mixing due to interaction between the protolunar disk and the Earth's atmosphere. In *Proc. 44th Lunar Planet. Sci. Conf.* 2566 (2013).
- Day, J. M. D. & Moynier, F. Evaporative fractionation of volatile stable isotopes and their bearing on the origin of the Moon. *Phil. Trans. R. Soc. A* 372, 20130259 (2014).
- 12. Visscher, C. & Fegley, B. Jr. Chemistry of impact-generated silicate melt-vapor debris disks. *Astrophys. J. Lett.* **767**, L12 (2013).
- Ward, W. R. On the vertical structure of the protolunar disk. Astrophys. J. 744, 140 (2012).
- 14. Thompson, C. & Stevenson, D. J. Gravitational instability in two-phase disks and the origin of the Moon. *Astrophys. J.* **333**, 452–481 (1988).
- Nakajima, M. & Stevenson, D. J. Investigation of the initial state of the Moon-forming disk: Bridging SPH simulations and hydrostatic models. *Icarus* 223, 259–267 (2014).
- 16. Ward, W. R. & Cameron, A. G. W. Disc evolution within the Roche limit. In *Proc. 9th Lunar Planet. Sci. Conf.* 1205–1207 (1978).
- 17. Ward, W. R. On the evolution of the protolunar disc. *Phil. Trans. R. Soc. A* 372, 20130250 (2014).
- Fegley, B. Jr & Cameron, A. G. W. A vaporization model for iron/silicate fractionation in the Mercury protoplanet. *Earth Planet. Sci. Lett.* 82, 207–222 (1987).
- 19. Schaefer, L. & Fegley, B. Jr. A thermodynamic model of high temperature lava vaporization on Io. *Icarus* 169, 216–241 (2004).

- Lodders, K. Solar system abundances and condensation temperatures of the elements. Astrophys. J. 591, 1220–1247 (2003).
- 21. Genda, H. & Abe, Y. Modification of a proto-lunar disk by hydrodynamic escape of silicate vapor. *Earth Planets Space* **55**, 53–57 (2003).
- Elkins-Tanton, L. T., Burgess, S. & Yin, Q.-Z. The lunar magma ocean: Reconciling the solidification process with lunar petrology and geochronology. Earth Planet. Sci. Lett. 304, 326–336 (2011).
- 23. Andrews-Hanna, J. C. *et al.* Ancient igneous intrusions and early expansion of the Moon revealed by GRAIL gravity gradiometry. *Science* **339**, 675–678 (2013).
- 24. Longhi, J. Experimental petrology and petrogenesis of mare volcanics. *Geochim. Cosmochim. Acta* **56**, 2235–2251 (1992).
- Hauri, E. H., Saal, A. E., Rutherford, M. J. & Van Orman, J. A. Water in the Moon's interior: Truth and consequences. *Earth Planet. Sci. Lett.* 409, 252–264 (2015).
- 26. Albaréde, F., Albalat, E. & Lee, C.-T. A. An intrinsic volatility scale relevant to the Earth and Moon and the status of water in the Moon. *Meteorol. Planet. Sci.* **50**, 568–577 (2015).

Acknowledgements

We thank D. Stevenson for comments and suggestions. Funding from NASA's Solar System Exploration Research Virtual Institute (SSERVI, for R.M.C., C.V. and J.S.), NASA's Lunar Advanced Science and Exploration Research Program (LASER, for R.M.C.), and from NSF's Planetary Astronomy Program (grant 1412175, for B.F.Jr) is gratefully acknowledged.

Author contributions

R.M.C. conceived the idea, integrated the component models, and wrote the paper. C.V. performed the chemical modelling and related analysis, J.S. performed the data analysis for the accretion models, and B.F.Jr provided the MAGMA model and relevant thermodynamic calculations for K, Na and Zn.

Additional information

Supplementary information is available in the online version of the paper. Reprints and permissions information is available online at www.nature.com/reprints. Correspondence and requests for materials should be addressed to R.M.C.

Competing financial interests

The authors declare no competing financial interests.

NATURE GEOSCIENCE DOI: 10.1038/NGE02574

LETTERS

Methods

This paper identifies a novel mechanism capable of explaining part or all of the Moon's volatile depletion pattern, evaluated through what is to our knowledge the first model to consider both the dynamical and thermodynamical evolution of the protolunar material as the Moon accretes after a giant impact. Each of the components of the model is based on current state-of-the-art, but nonetheless still represents an approximated description, as discussed in more detail below. The observed depletions that would result from the proposed mechanism depend primarily on the extent of mixing in the Moon's interior, as discussed above; this is uncertain and merits further consideration.

Dynamical model. We use results from an accretion model^{6,7} that considers a uniform surface density (σ_T) disk interior to the Roche limit and a condensate outer disk described by an N-body accretion simulation. In reality, σ_T would vary with radius, but T_c varies rather weakly with σ_T (see equation (3) below) as the Moon accretes substantial inner disk material. The model^{6,7} assumes the inner disk maintains a silicate two-phase state until its mass drops below 0.2 lunar masses, comparable to the condition (0.14 lunar masses, see below) obtained with a more realistic treatment¹⁷ with separately evolving melt and vapour phases and radially varying surface densities. Canonical impacts produce primarily condensed outer disks^{1,15}, consistent with the first consideration. However recent alternatives^{15,27,28} produce highly vaporized disks. In these cases, outer disk vapour might condense over approximately a decade in the absence of local viscous heating, and this timescale could still be shorter than the inner disk lifetime (\sim 10² yr), leading to a similar overall evolution. However, the initial evolution of a highly vaporized disk remains uncertain and different evolutions are conceivable²¹.

We consider that, in the inner disk, tidal disruption of clumps produces a viscosity 16 $v \approx \pi^2 G^2 \sigma_m^2/\Omega^3$, where σ_m is the melt surface density, $\Omega = \sqrt{G M_{\bigoplus}/r^3}$ is orbital frequency, G is the gravitational constant, M_{\bigoplus} is the Earth's mass, and r is the orbital radius. The Moon's accretion may be characterized by three stages 6 . Condensed material outside the Roche limit rapidly accretes into a moonlet(s) ('phase 1' in Fig. 1a). Moonlets that accrete in the outer disk interact with the inner disk through resonant torques, which cause their orbits to expand while opposing the outward viscous diffusion of the inner disk 67,17 . A nearby moonlet becomes able to confine the inner disk's outer edge to within the Roche limit once the moonlet's mass exceeds $O(10^{-1})$ lunar masses 67,17 , which initially shuts off its accretion of inner disk material ('phase 2' in Fig. 1a). As the moonlet's orbit expands, its resonances leave the disk and the inner disk is freed to spread. As inner disk melt spreads beyond the Roche limit, it forms large clumps through local gravitational instability that can be accreted by the growing moon(s) or scattered back into the inner disk or onto the Earth ('phase 3' in Fig. 1a) 67 .

The volatile depletion mechanism identified here occurs during phase 3, when the Moon acquires up to about half of its mass from clumps formed at the Roche limit. Such a phase will occur so long as, once the Moon's accumulation commences, the timescale for accretion of material outside the Roche limit is short compared to the lifetime of the inner disk. This seems a good assumption for disks produced by canonical impacts^{1,15}, and perhaps for disks produced by high-angular-momentum impacts 15,27,28, although the latter might evolve substantially before the commencement of accretion. Our model assumes that, during this final phase of the Moon's growth, the dominant source of viscosity in the inner disk is associated with the melt, so that melt is driven radially outwards whereas inner disk vapour stays largely in place until it condenses^{17,29}. It is, however, possible that the vapour could be viscous, and vapour that spread outwards during phase 3 and subsequently condensed in the cooler outer disk could (depending on the radial distance travelled before condensation) add volatile-rich material to the Moon that is not accounted for in our model. Viscosity in a gas disk is often parameterized as $v_{\rm gas}\!=\!\alpha_{\rm g}c^2/\Omega$, where $\alpha_{\rm g}$ is a dimensionless parameter and c is the sound speed. Laboratory estimates suggest that hydrodynamic turbulence due to Keplerian shear produces $\alpha_g < 10^{-5}$; such a low α_g would imply a vapour mass flux across the Roche limit substantially smaller than the flux of melt due to the instability-induced viscosity considered here. Efficient diffusive mixing between the disk's vapour and the Earth's silicate vapour atmosphere has been proposed as a means to equilibrate Earth-Moon isotopic compositions³²; this mechanism requires the mixing be accompanied by minimal angular momentum transport³³, also implying a small effective α_{σ} . A large vapour viscosity, with $\alpha_{\rm g} \sim O(10^{-2})$, would be associated with active magneto-rotational instability (MRI), but this could be difficult to achieve in a two-phase protolunar disk where orbital frequencies are high and ongoing condensation/settling of silicates (as well as more refractory grains) would tend to reduce the disk ionization fraction34.

Thermal model. We assume an initial inner disk that is regulated by the silicate two-phase equilibrium 13,14,17 , with a photospheric temperature $T_{\rm ph} \sim 2,000~{\rm K}$ and $T_{\rm c}$ given by equation (1) for a given $(\sigma_T,x_{\rm c})$. The time evolution of σ_T is provided by the accretion model. We consider a range of plausible $x_{\rm c}$ values motivated by protolunar disk models 13,14,17,29 . After the giant impact, the inner disk may adjust rapidly to a state in which there is local vertical thermal balance between viscous

dissipation, release of latent heat due to condensation, and radiative cooling from the photosphere 13,14,17. In a two-phase silicate disk, this can be accomplished through either 13,17 a vertically well-mixed disk with a very low gas mass fraction, in which the two-phase sound speed is regulated to the point of marginal instability (implying $x_c \sim O(10^{-2})$, refs 13,14), or a vertically stratified disk, in which the surface density of a gravitationally unstable mid-plane melt layer adjusts itself through condensation or evaporation until thermal balance is achieved^{13,17}. The second, vertically stratified, case implies a total magma layer mass of about 0.14 lunar masses, with the remainder of the inner disk mass contained in an overlying vapour-rich atmosphere with $O(10^{-1}) \le x_c \le 1$ (refs 13,17). This case may be more likely, owing to rapid settling of melt droplets to the mid-plane 13,17,29. The assumption of two-phase equilibrium implies an intimate mixture of gas and liquid, including in the mid-plane, that is, $x_c > 0$. This is probable in the region near the Roche limit, because gravitational stirring by temporary instability-induced clumps will maintain a finite melt layer thickness and a corresponding spatial density of melt much less than the density of a continuous fluid 16,29, implying dispersed clumps and droplets with intervening vapour-filled space.

We consider that instability-induced clumps will form near the disk mid-plane at temperature T_c . Silicate droplets will condense at altitude, but settle rapidly while still small²⁹. For relevant values of σ_T (between 10^6 and few $\times 10^7$ g cm⁻²), we find that T_c from equation (1) is well approximated by (see Supplementary Fig. 4)

$$T_{\rm c} \approx T_{\rm I} \left(\frac{\sigma_T}{10^7 \, {\rm g \, cm^{-2}}} \right)^{\alpha} \tag{3}$$

where T_1 and α are fitting factors, with T_1 = 3,560 K and α = 0.063 for x_c = 0.01, T_1 = 3,740 K and α = 0.065 for x_c = 0.1, and T_1 = 4,010 K and α = 0.07 for x_c = 1. The appropriate value for x_c near the Roche limit may evolve with time. Thus the mid-plane temperature evolution would be expected to lie between the x_c = 0.01 and x_c = 1 curves in Fig. 3b. Equations (1) and (3) ignore heating by the Earth. After the giant impact, Earth's atmosphere may rapidly adjust to a radiating temperature 14 $T_{\oplus} \sim 2,000$ to 2,500 K. Because the planet's luminosity decreases as approximately $(1/r)^2$ and $T_{\oplus} \sim T_{\rm ph}$ while the disk is in a two-phase silicate state, Earth shine is a minor influence on the disk's temperature near the Roche limit during this phase.

We assume the inner disk's silicate vapour fully condenses once $\sigma_T < 1.7 \times 10^6 \ \mathrm{g \ cm^{-2}}$, as in ref. 6. Subsequently we estimate T_{ph} assuming a balance between viscous dissipation in the mid-plane (with rate per area $\dot{E}_v = 9\sigma_m v \Omega^2/4$), Earth shine on the upper and lower surfaces of the disk's volatile-rich atmosphere (with rate per area \dot{E}_{CP}), and radiative cooling from these surfaces, with

$$2\sigma_{\rm SB}T_{\rm ph}^4 = \dot{E}_{\oplus} + \dot{E}_{\rm v} \approx 2\sigma_{\rm SB}T_{\oplus}^4 \left[\frac{2}{3\pi} \left(\frac{R_{\oplus}}{r}\right)^3\right]$$

$$+ \frac{1}{2} \left(\frac{R_{\oplus}}{r} \right)^2 \left(\frac{3 - \beta}{2} - 1 \right) \left(\frac{c}{r \Omega} \right) + \frac{9\pi^2 G^2 \sigma_m^3}{4\Omega}$$
 (4)

where $\sigma_{\rm SB}$ is the Stefan–Boltzmann constant, $T_{\rm c}(r) \propto (1/r)^{\beta}$, implying an atmosphere scale height that increases with radius as $H \propto r^{3/2-(\beta/2)}$, and the expression for \dot{E}_{\bigoplus} is taken from Equation B4 in ref. 35. A corresponding estimate for $T_{\rm c}$ is 36

$$2\sigma_{\rm SB}T_{\rm c}^4 \approx \left(1 + \frac{3}{8}\kappa\sigma_{\rm v}\right)\dot{E}_{\rm v} + \dot{E}_{\bigoplus} \tag{5}$$

For $\sigma_T \sim 10^6$ g cm⁻² (that is, the later evolution in Fig. 3) and an anhydrous BSE-composition disk¹², expected vapour surface densities are $\sigma_v \sim 10^4$ g cm⁻² to 10^3 g cm⁻² as the disk cools from \sim 3,000 K to \sim 1,800 K (see Supplementary Fig. 5). An additional 1,000 ppm H₂O would provide up to $\sigma_v \sim 10^{-3}\sigma_T$ g cm⁻² across this temperature range¹², or $\sigma_v \sim 10^3$ g cm⁻² for $\sigma_T \sim 10^6$ g cm⁻². Either implies $\sigma_v \ll \sigma_m \approx \sigma_T$ in the disk's later phase. The atmospheric opacity κ is uncertain, with $\kappa \sim 10^{-2}$ cm² g⁻¹ estimated for relevant densities and temperatures for a solar composition gas³⁷. In Fig. 3b, we simply set $(\kappa \sigma_v) = 10$. In the case of a much higher opacity (such as would apply if silicate droplets contribute significantly), the implied temperature gradient from (5) would be super-adiabatic, and in this case the vertical heat flux would be convectively rather than radiatively transported, resulting in an adiabatic temperature gradient¹³. Our conclusions are not sensitive to the treatment of T_c in this phase, since by this time the Moon has essentially completed its accretion.

Chemical model. The MAGMA code 12 is used to calculate for a given T_c the partial pressure of each gas species i (P_i) in equilibrium with the multicomponent silicate melt, with $P_i = x_i P_T$, where x_i is the mole fraction abundance of each gas and P_T is the total pressure. We relate the partial pressure of each species to its vapour surface density $(\sigma_{i,v})$ as $P_i = \rho_i R T_c / \mu_i \approx \sigma_{i,v} R T_c / (2H \mu_i)$, where ρ_i and μ_i are the vapour density and molecular weight of species i, and $H \approx \sqrt{2} c/\Omega$ is the disk's scale height, with sound speed $c = \sqrt{\gamma R T_c / \mu_i}$, mean atmospheric adiabatic

LETTERS NATURE GEOSCIENCE DOI: 10.1038/NGE02574

index and molecular weight, $\overline{\gamma}$ and $\overline{\mu}$, and Ω calculated at the Roche limit. The vapour surface density of each gas species and the total vapour surface density are

$$\sigma_{i,v} \approx \frac{2P_i \mu_i}{\Omega} \sqrt{\frac{2\overline{\gamma}}{R T_c \overline{\mu}}}; \quad \sigma_v \approx \frac{2P_T}{\Omega} \sqrt{\frac{2\overline{\gamma} \overline{\mu}}{R T_c}}$$
 (6)

where $\sigma_v = \sum_i \sigma_{i,v}$ given $P_T = \sum_i P_i$.

The total vapour density for each element is determined by adding the contributions of each gas species i containing element M,

$$\sigma_{M,v} = \sum_{i} \frac{n_{M(i)} \mu_M}{\mu_i} \sigma_{i,v} \tag{7}$$

where μ_M is the atomic weight of element M and $n_{M(i)}$ is the stoichiometric coefficient for element M in species i ($n_{\mathrm{Si(SiO_2)}}=1, n_{O(\mathrm{SiO_2})}=2$, and so on). Once element vapour densities are known, the relative fraction of each element in vapour versus melt can be determined for a given total surface density of melt and vapour. The bulk inventory of each element is given by $\sigma_M = w_M \sigma_T$, where σ_M is the total surface density (melt + vapour) of element M, w_M is the mass fraction of element M in the system, and σ_T is the total surface density of the melt and vapour disk ($\sigma_T = \sigma_M + \sigma_v$). The mass fraction of each element that is vaporized is $m_{\mathrm{vap}} = \sigma_{\mathrm{Mv}} / \sigma_M$.

MAGMA assumes a melt phase is always present—in other words, that there is in effect an inexhaustible supply of BSE-composition material. Without modification, this would lead to unrealistically large estimates for σ_v and P_T for the situation considered here, in which there is a finite local supply of melt. As such we impose the additional requirement that $\sigma_{M,v} < \sigma_{M}$ —that is, that the vapour surface density for each element (and therefore its partial pressure per equation (6)) has a maximum value set by the element's total (bulk) inventory in the disk. This can be seen in Fig. 2a and Supplementary Fig. 5, where the estimated vapour density of each element increases with temperature until $\sigma_{M,v} \approx \sigma_M$, whereupon the density remains constant. We approximate T_{50} as the temperature at which $\sigma_{M,v} = 0.5\sigma_M = 0.5w_M\sigma_T$, so that T_{50} is ultimately a function of melt-vapour equilibria (and therefore T_c), the bulk element inventory (assumed here to correspond to a BSE composition), and the disk surface density. Resulting condensation temperatures are approximations, but should provide reasonable estimates for the expected behaviour. Our predicted T_{50} values for Na and K are broadly similar to those recently reported for Na and K using a different

approach³⁸, particularly for the regime of interest as the Moon accretes inner disk material ($\sigma_T > 10^6 \text{ g cm}^{-2}$ and more than approximately a few bar in pressure).

Code and Data Availability. The SyMBA *N*-body accretion code is a freely available extension to the SWIFT package (https://www.boulder.swri.edu/~hal/swift.html). Modifications made to SyMBA to model lunar accretion are described in detail in ref. 6. The MAGMA code is distributed on request (contact B. Fegley), subject to the requirement that publications using it cite the two papers describing the code (refs 18,19). Data shown in Figs 1–3 is available on request.

References

- 27. Ćuk, M. & Stewart, S. T. Making the Moon from a fast-spinning earth: A giant impact followed by resonant despinning. *Science* **338**, 1047–1052 (2012).
- 28. Canup, R. M. Forming a Moon with an Earth-like composition via a giant impact. *Science* **338**, 1052–1055 (2012).
- Machida, R. & Abe, Y. The evolution of an impact-generated partially vaporized circumplanetary disk. Astrophys. J. 617, 633–644 (2004).
- 30. Ji, H., Burin, M., Schartman, E. & Goodman, J. Hydrodynamic turbulence cannot transport angular momentum effectively in astrophysical disks. *Nature* **444**, 343–346 (2006).
- Edlund, E. M. & Ji, H. Nonlinear stability of laboratory quasi-Keplerian flows. Phys. Rev. E 89, 021004 (2014).
- 32. Pahlevan, K. & Stevenson, D. J. Equilibration in the aftermath of the lunar-forming giant impact. *Earth Planet. Sci. Lett.* **262**, 438–449 (2007).
- 33. Melosh, H. J. New approaches to the Moon's isotopic crisis. *Phil. Trans. R. Soc. A* **372**, 20130168 (2014).
- Fujii, Y. I., Okuzumi, S., Tanigawa, T. & Inutsuka, S. On the viability of the magnetorotational instability in circumplanetary disks. *Astrophys. J.* 785, 101 (2014).
- Ruden, S. P. & Pollack, J. B. The dynamical evolution of the protosolar nebula. Astrophys. J. 375, 740–760 (1991).
- Nakamoto, T. & Nakagawa, Y. Formation, early evolution, and gravitational stability of protoplanetary disks. Astrophys. J. 421, 640–650 (1994).
- Marigo, P. & Aringer, B. Low-temeprature gas opacity. Astrono. Astrophys. 508, 1539–1569 (2009).
- 38. Petaev, M. I., Jacobsen, S. B. & Huang, S. Testing models of the Moon's origin, II: Phase relation in a proto-lunar disk of the BSE composition. In *Proc.* 46th Lunar Planet. Sci. Conf. 2245 (2015).